

Infrared spectroscopy of synthetic and natural stishovite

A. M. HOFMEISTER

Department of Geology, University of California, Davis, California 95616, U.S.A.

J. XU

Department of Geology and Geophysics, University of Hawaii, Honolulu, Hawaii 96822, U.S.A.

S. AKIMOTO

Institute for Study of the Earth's Interior, Okayama University, Misasa, Tottori-ken, 682-02 Japan

ABSTRACT

Single-crystal and polycrystalline reflectance and thin-film absorption infrared spectra for synthetic stishovite exhibit a pattern characteristic of the rutile structure. Three E_u LO-TO fundamentals were observed at 1020–820, 700–580, and 565–470 cm^{-1} , and one A_{2u} mode was found at 950–675 cm^{-1} . These values are considerably higher than frequencies of other rutile-type compounds and cannot be predicted from TiO_2 spectra using simple mass/bond-length considerations. The LO-TO range of the highest energy Si-O octahedral stretch overlaps considerably with that of Si-O tetrahedral stretches in orthosilicates from 1060–850 cm^{-1} and in tectosilicates from 1250–950 cm^{-1} . This relationship implies that frequency alone is insufficient to establish coordination numbers for Si. Natural stishovite from Meteor Crater, Arizona, has fundamentals similar to those of synthetic samples and an additional strong feature near 740 cm^{-1} . Excess bands in both IR and Raman spectra are best explained by $(\text{SiF}_6)^{2-}$ contamination. The IR data indicate an ordered structure that is free of SiO_2 glass impurities.

INTRODUCTION

Characterization of the thermodynamic properties of minerals at pressure requires intimate knowledge of their vibrational properties. Stishovite has been problematic in that previous infrared spectra are inconsistent with expectations for the ideal rutile structure (e.g., Kieffer, 1979). Raman spectra show that synthetic stishovite possesses the rutile structure, although the origin of the extra bands in the natural sample has not been entirely resolved (Hemley et al., 1986). This study completes the infrared characterization at 1 atm of synthetic and natural stishovite. Companion papers will establish frequencies of the three inactive bands by comparing vibrational data for SiO_2 with that of other compounds having the rutile structure (Hofmeister et al., in preparation a), and calculate bulk moduli (Hofmeister, in preparation a) and heat capacity (in preparation b).

EXPERIMENTAL

Infrared spectra were obtained from three samples. The single crystal of stishovite synthesized by Sinclair and Ringwood (1978) has dimensions of about $10 \times 40 \times 100 \mu\text{m}$. Detailed descriptions are given by Weidner et al. (1982) and Hill et al. (1983). Polycrystalline stishovite

synthesized at 95 kbar and 1100 °C contains small amounts of graphite (Hemley et al., 1986). Polycrystalline natural samples were extracted from Coconino sandstone using concentrated HF and HCl (Fahey, 1964); extractions were repeated to remove impurities (Hemley et al., 1986).

Infrared spectra were obtained using a Nicolet 7199 optical bench and 1280 data processor, and a Spectra-tek FTIR microscope. Far-IR spectra were obtained at 4 cm^{-1} resolution from 400 to 70 cm^{-1} using a Ge-bolometer. Mid-IR spectra were obtained at 1 cm^{-1} resolution above 400 cm^{-1} using a HgCdTe detector. Reflection spectra were measured both from powder dispersed over a 300- μm diameter area (20 000 scans) and from the largest face of the single crystal (over 250 000 scans). Because of the small sample size and its specific geometry, polarized measurements were not feasible. Absorption spectra were collected from a polycrystalline sample that had been compressed into a thin film (ca. 0.5 to 2 μm) by a diamond anvil cell.

VIBRATIONAL SPECTROSCOPY

The number of vibrations in the rutile-type structure (space group $P4_2/mnm$ or D_{4h}^{14} with $Z = 2$) is predicted by

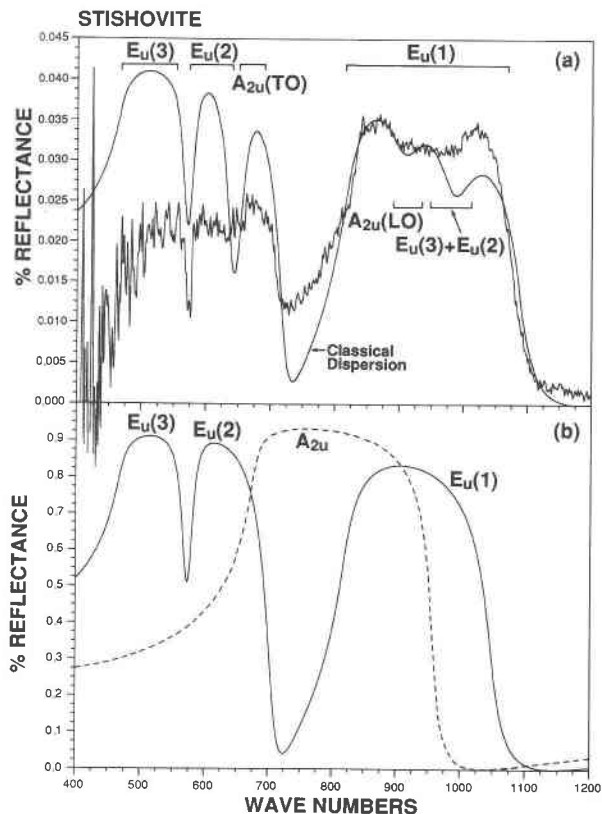


Fig. 1. Single-crystal IR spectra of synthetic stishovite. (a) Heavy line, raw unpolarized reflectance data. The noise level is high owing to the small size and the lack of a highly polished surface. The three strong peaks are from E_u . The features at ~ 650 and 950 cm^{-1} are A_{2u} . Light line, classical dispersion fit to the data using three E_u peaks, two A_{2u} components, and a combination band at high energy. (b) Synthetic E_u (solid) and A_{2u} (dashed) spectra derived from the classical dispersion analysis of the reflection data. Parameters given in text and Table 2. The LO positions are $12\text{--}35 \text{ cm}^{-1}$ lower than those in the raw spectra.

symmetry as $A_{1g}(R) + A_{2g} + B_{1g}(R) + B_{2g}(R) + E_g(R) + 2B_{1u} + A_{2u}(IR) + 3E_u(IR)$, where R indicates Raman active bands and IR indicates infrared active bands. This result cannot be subdivided into internal or external modes because rutile lacks isolated structural units. Analysis of the dynamical matrix (force constants) allows description of the modes at zone center in terms of relative displacements (Dayal, 1950). Pictures are given by Traylor et al. (1971). All IR modes are cation-anion stretching motions.

The IR data corroborate the X-ray diffraction (Sinclair and Ringwood, 1978) and Raman (Hemley et al., 1986) results, which show that stishovite crystallizes in the ideal rutile structure because the unpolarized reflectance infrared spectrum of synthetic single-crystal stishovite (Fig. 1a) has the three strong E_u peaks, as predicted by the symmetry analysis. Additional weak peaks are present owing to polarization mixing. Kramers-Kronig analysis was attempted but did not give acceptable results. A de-

TABLE 1. Infrared peak positions (cm^{-1}) of stishovite

	Reflectance	Classical dispersion	Powder reflectance	Thin film
$E_u(3)$	565– ~ 450	568–470	540–478	530– ~ 470
$E_u(2)$	$\sim 650\text{--}578$	706–580	610–575	$\sim 625\text{--}580$
A_{2u}	950 } 900 } {705 650	$\sim 910\text{--}\sim 650$	950–670	960–763*
$E_u(1)$	1075 } 800 }	1047–820	1020–832	1020–836

* Taken from extrapolation of A_{2u} peak to zero pressure.

tailed description of the mathematics of this procedure is given by Hofmeister et al. (in preparation b). The difficulties can be traced to low absolute values of reflectance owing to the poor polish on the crystal and to a low signal-to-noise ratio that could not be further improved by signal averaging, owing to the small sample size. Furthermore, polarization mixing complicates the spectrum considerably and can lead to incorrect mode parameters (e.g., Kahan et al., 1971). Therefore, peak positions were approximated by several other methods, as follows.

Peak positions taken directly from the reflectance spectrum (i.e., at half height on each side of the band), as listed in Table 1, were established by comparing our spectra (Fig. 1a) with the pure spectra of GeO_2 having the rutile structure (Roessler and Albers, 1972) and with spectra of GeO_2 altered by polarization mixing (Kahan et al., 1971). Polarization mixing causes separation of the broad A_{2u} mode into its LO and TO components (Hofmeister et al., in preparation a) because of the mathematical requirement that the TO modes must alternate with LO modes (Scott and Porto, 1967). Thus, both the mixed GeO_2 spectrum (Kahan et al., 1971) and SiO_2 (Fig. 1a) have three bands at low frequency owing to the $E_u(3)$, $E_u(2)$, and $A_{2u}(\text{TO})$ modes. At high frequency, a distinct doublet is seen in mixed GeO_2 : Hofmeister et al. (in preparation a) attribute this to the accidental degeneracy of the combination mode [$E_u(3) + E_u(2)$] with the LO component of A_{2u} . The mixed GeO_2 spectra contains a “reversed” mode, as quartz does (Scott and Porto, 1967). We interpret the structure of SiO_2 at high frequency (Fig. 1a) as $E_u(1)$ containing two weak, but not degenerate, modes: i.e., $A_{2u}(\text{LO})$ and the combination mode (which should be slightly less than the sum of its fundamentals at 1050 cm^{-1} ; its proximity to $E_u(\text{LO})$ is expected to enhance the combination’s intensity). The frequency of $A_{2u}(\text{LO})$ is always slightly less than that of $E_u(\text{LO})$ (Hofmeister et al., in preparation a). Therefore, $A_{2u}(\text{LO})$ must be at 900 to 1000 cm^{-1} . Lastly, the $E_u(1)$ LO component in the mixed GeO_2 spectrum occurs at 50 cm^{-1} higher than in the pure spectrum, so that $E_u(1)$ LO of SiO_2 derived directly from reflectance data may be high by a like amount.

Our inferences can be assessed by using classical dispersion analysis (e.g., Spitzer et al., 1962) to construct synthetic spectra from a set of TO peak positions, full widths at half height γ , and oscillator strengths f . Initial

TABLE 2. Comparison to other oxides in the rutile structure

	SiO ₂ expt.*	SiO ₂ model**	SiO ₂ eqn. 1	GeO ₂ expt.†	SnO ₂ expt.‡	TiO ₂ expt.§
E _u	565–470	503	478–241	345–300	276–244	374–189
γ	20			9.0	6.1(7.8)	19
f	8.8			6.9	4.6(5.8)	78
E _u	700–580	552	547–495	470–370	366–293	428–388
γ	15			7.4	9.4(6.3)	12
f	0.44			1.88	2.6(1.3)	2
A _{2u}	950–675	609	1035–221	755–455	705–477	811–173
γ	15			15.9	13.8(18.6)	—
f	4.0			7.8	5.4(5.4)	—
E _u	1020–820	812	1074–630	815–635	770–618	841–494
γ	30			19.1	30.9(20.6)	12
f	1			1.6	2.1(1.6)	2

* Uncertainties are ± 5 cm⁻¹ except for TO of E_u(1), which is ± 1 cm⁻¹, and A_{2u}(3), which is ± 10 cm⁻¹.

** Striefer and Barsch (1976).

† Hofmeister et al. (in preparation b); Roessler and Albers (1972).

‡ Katiyar et al. (1971); numbers in parentheses are from Summit (1968).

§ Traylor et al. (1971); Spitzer et al. (1962).

values of the TO positions were taken from reflectance data, and widths and strengths were estimated from classical dispersion analyses of other oxides with the rutile structure (Table 2). A good fit for the spectrum was obtained for three E_u peaks (given in Table 2), two components for A_{2u} (TO = 650 cm⁻¹, γ = 20 cm⁻¹, f = 0.2; LO = 910, γ = 60, f = 0.07) and the combination band (ν = 990, γ = 60, f = 0.035). The synthetic reflectance spectrum (Fig. 1a) supports our inference that the two "ears" on the broad high-energy peak for the measured spectrum are connected with the superposition of the weaker A_{2u}(LO) component and the combination mode on E_u(1), and that the rise at high frequency on the middle peak is due to A_{2u}(TO).

The inferred polarized spectra (Fig. 1b) are remarkably similar to those of other oxides in the rutile structure (see Table 2). The relationship of the calculated E_u polarization (Fig. 1b) to the unpolarized stishovite spectrum (Fig. 1a) mimics that between the GeO₂ measurements of Roessler and Albers (1972) and Kahan et al. (1971).

The reflectance spectrum from polycrystalline synthetic stishovite shows essentially the same features (Fig. 2a). Separate peaks occur at the TO and LO positions because of scattering and absorption from the small grains and irregular surface. Weak bands at 670 and 950 cm⁻¹ for the A_{2u} mode corroborate our classical dispersion analysis, as do the relative intensities of the three E_u components.

Far-IR spectra taken from thin films of the polycrystalline synthetic contained no bands. Mid-IR absorption spectra (Fig. 2b) have the same three E_u peaks, with a shoulder at about 763 cm⁻¹ that is attributed to A_{2u}. This shoulder becomes prominent as the pressure is increased because its slope (dν/dP) differs from that of the neighboring E_u band (Hofmeister et al., in preparation c). The frequency for A_{2u} in thin film measurements of SiO₂ is considerably higher than its TO position derived from reflection, as is the case for GeO₂ (Hofmeister et al., in

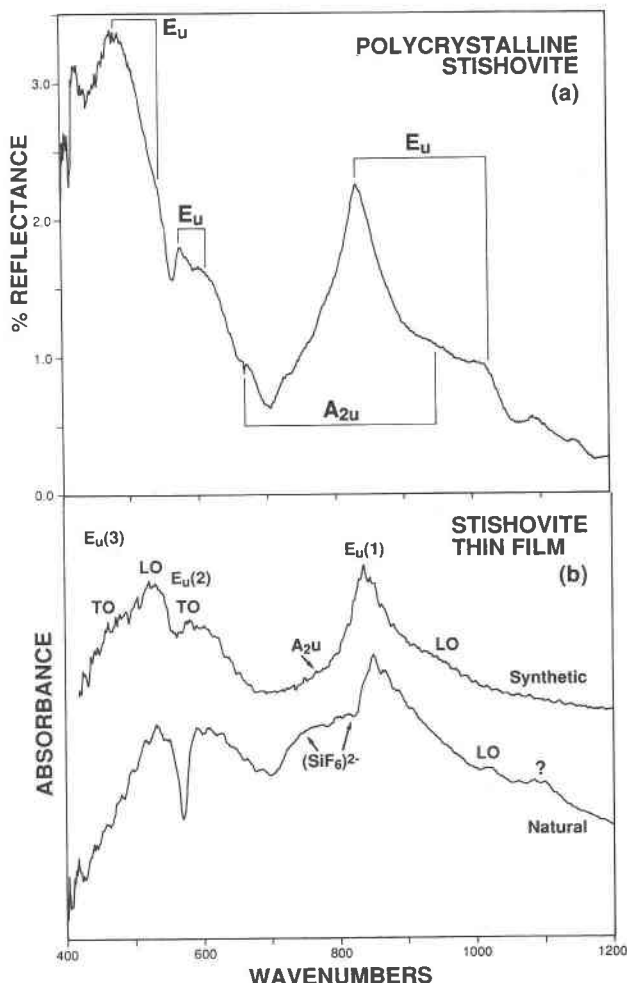


Fig. 2. (a) Unpolarized reflectance spectrum measured from polycrystalline synthetic stishovite dispersed over an area 300 μm across. Strong absorption features are present because of scattering among the microcrystals. The 425 cm⁻¹ band is an artifact owing to noise near the cutoff frequency. The relative peak heights support the correctness of oscillator strengths used in the classical dispersion analysis. (b) Unpolarized thin film spectra of natural and synthetic stishovite. Natural samples have additional bands at 730–800 cm⁻¹. The large intensity in the 800 cm⁻¹ region of the natural sample probably causes the apparent shift of the uppermost band to higher energies.

preparation a). This effect is attributed to the breadth of the mode. LO modes are observed in thin films because light passing through the diamond anvil cell strikes the sample at angles ranging up to about 15°, and the sample is not sufficiently thin or is wedged (Berreman, 1963).

Peak positions listed in Table 1 from the raw and analyzed data for the three measurements are generally in good agreement. The most accurate positions are compiled in Table 2. The values are spread over a moderate range for silicates (470–1020 cm⁻¹).

Spectra from natural stishovite exhibit the same four fundamentals at approximately the same intensities as the two synthetic samples but have an additional strong

feature from 730 to 830 cm^{-1} (Fig. 2b) and show better resolution between the two low-energy E_u bands. The weak peaks at 1020 and 1100 cm^{-1} for the natural sample are also present in the reflectance from the synthetic polycrystals (Fig. 2a). The Raman spectrum of the same sample has an additional broad band at 450 cm^{-1} and additional weak bands at 900–1000 cm^{-1} (Hemley et al., 1986). Previous powder IR spectra of natural stishovite also show several bands in the far-IR at 330, 285, and possibly 220 cm^{-1} (Kieffer, 1979) and resemble the thin-film spectra (Lyon, 1962), except that the peak positions are sharper and are shifted to higher frequencies owing to the KBr technique.

DISCUSSION

A likely candidate for the origin of the extra bands in natural stishovite from Meteor Crater is contamination by $(\text{SiF}_6)^{2-}$ that is charge-compensated by alkali ions. This proposal is supported by the following observations. (1) Octahedral Si-F vibrations occur at 741 and 483 cm^{-1} in IR spectra and 663, 447, and 408 cm^{-1} in Raman spectra (Begun and Rutenberg, 1967). These positions are essentially the same as the intense extra bands seen in natural samples. (2) Peaks corresponding to translations of alkali ions frequently occur in the far-IR, and with low intensities (e.g., Moenke, 1974), and are consistent with the presence of multiple, weak far-IR bands in natural stishovite. (3) Treatment with strong acids could yield some surface exchange of O^{2-} with F^- and could easily extract alkalis from feldspar in the Coconino sandstone for later deposition in defects on the surface of stishovite crystals. (4) Surface modes in such fine-grained polycrystalline samples are expected to perturb the IR spectrum, resulting in high intensity bands.

The positions of the impurity bands in IR data are not consistent with significant contamination with SiO_2 glass because the glass typically has two bands at 1100 and 800 cm^{-1} , which definitely were not observed in the infrared spectrum. Weak shoulders near 800 cm^{-1} and very high frequency are probably connected with graphite impurities detected by Hemley et al. (1986). We suggest that glass could be produced through laser heating in the Raman experiments. In addition, it is not likely that the excess bands originate through disorder because the natural sample has higher resolution, as indicated by the separation between the LO component of $E_u(3)$ from the TO component of $E_u(2)$; this implies that natural samples could be more ordered than synthetic.

IR frequencies for stishovite are considerably higher than those of the other oxides (Table 2), as is expected, since stishovite has the lightest mass and shortest metal-oxygen bond distance of the four compounds. Frequencies of SiO_2 may be predicted from rutile spectra through the relationship derived by Batsanov and Derbeneva (1969):

$$\frac{\nu_s}{\nu_r} = \left(\frac{d_r^3 \mu_s}{d_s^3 \mu_r} \right)^{1/2} \quad (1)$$

where μ is the reduced mass, d the average cation-oxygen bond length, and r and s denote rutile and stishovite, respectively. For stishovite, d_s is the average bond length of 1.774 Å (Hill et al., 1983); for rutile, d_r is 1.983 Å (Wyckoff, 1965). The discrepancies are large (Table 2), indicating that rutile is not a good model for stishovite. Neither are rigid ion calculations for stishovite particularly close: Striefler and Barsch's (1976) model values are low, but within 3 to 20% of the measured TO values (Table 2). Approximately the same accuracy was attained in predicting the Raman bands observed by Hemley et al. (1986). However, quasilinear trends exist for various IR and Raman frequencies with cell volume for oxides and fluorides having the rutile structure (Hofmeister et al., in preparation a), which can be used to predict the three inactive modes with confidence.

It is of interest to compare stishovite spectra with that of other compounds containing octahedrally coordinated Si. MgSiO_3 with the ilmenite structure has LO-TO stretching vibrations at 940–740, 740–720, and 720–658 cm^{-1} (Hofmeister, in preparation b). These values are somewhat lower than that of the highest-energy E_u band in stishovite at 1020–832 cm^{-1} , which is an Si-O stretch. The range of Si-O octahedral stretches (LO and TO) involves much higher energies than commonly assumed and overlaps considerably with Si-O tetrahedral (LO and TO) stretches from 1060–850 cm^{-1} in orthosilicates (Hofmeister, 1987; Hofmeister et al., in preparation b) and from 1250–950 cm^{-1} in tectosilicates (Moenke, 1974). Thus, frequency alone is insufficient reason to assign a band as an octahedral Si-O stretch.

ACKNOWLEDGMENTS

We thank P. Aruscavage for the extractions and E.C.T. Chao (USGS) for use of the natural samples. Spectra were collected at the Geophysical Laboratory. Support was provided by NSF grants EAR-8419984 and EAR-8816531 and by a fellowship in science and engineering from the David and Lucile Packard Foundation to AMH. Reviews by R.J. Hemley (Geophysical Laboratory) and W. White (Pennsylvania State University) substantially improved the manuscript.

REFERENCES CITED

- Batsanov, S.S., and Derbeneva, S.S. (1969) Effect of valency and coordination of atoms on position and form of infrared absorption bands in inorganic compounds. *Journal of Structural Chemistry (USSR)*, 10, 510–515.
- Begun, G.M., and Rutenberg, A.C. (1967) Vibrational frequencies and force constants of some group IVa and group Va hexafluoride ions. *Inorganic Chemistry*, 6, 2212–2216.
- Berreman, R.G. (1963) Infrared absorption at longitudinal optic frequency in cubic crystal films. *Physical Review*, 130, 2193–2198.
- Dayal, B. (1950) The vibration spectrum of rutile. *Proceedings of the Indian Academy of Science*, A32, 304–312.
- Fahey, J.J. (1964) Recovery of coesite and stishovite from Coconino sandstone of Meteor Crater, Arizona. *American Mineralogist*, 49, 1643–1647.
- Hemley, R.J., Mao, H.K., and Chao, E.C.T. (1986) Raman spectrum of natural and synthetic stishovite. *Physics and Chemistry of Minerals*, 13, 285–290.
- Hill, R.J., Newton, M.D., and Gibbs, G.V. (1983) A chemical study of stishovite. *Journal of Solid State Chemistry*, 47, 185–200.
- Hofmeister, A.M. (1987) Single-crystal absorption and reflection infrared

- spectroscopy of forsterite and fayalite. *Physics and Chemistry of Minerals*, 14, 499–513.
- Kahan, A., Goodrum, J.W., Singh, R.S., and Mitra, S.S. (1971) Polarized reflectivity spectra of tetragonal GeO_2 . *Journal of Applied Physics*, 42, 4444–4446.
- Katiyar, R.S., Dawson, P., Hargreave, M.M., and Wilkinson, G.R. (1971) Dynamics of the rutile structure III. Lattice dynamics, infrared and Raman spectra of SnO_2 . *Journal of Physics C: Solid State Physics*, 4, 2421–2431.
- Kieffer, S.W. (1979) Thermodynamics and lattice vibrations of minerals, 2: Vibrational characteristics of silicates. *Reviews of Geophysics and Space Physics*, 17, 20–34.
- Lyon, R.J.P. (1962) Infra-red confirmation of six-fold coordination of silicon in stishovite. *Nature*, 196, 266–267.
- Moenke, H.H.W. (1974) Silica, the three-dimensional silicates, borosilicates, and beryllium silicates. In V.C. Farmer, Ed., *The infrared spectra of minerals*, p. 365–382, Mineralogical Society, London.
- Roessler, D.M., and Albers, W.A.J. (1972) Infrared reflectance of single crystal tetragonal GeO_2 . *Journal of the Physics and Chemistry of Solids*, 33, 293–296.
- Scott, J.F., and Porto, S.P.S. (1967) Longitudinal and transverse optical lattice vibrations in quartz. *Physical Review*, 161, 903–910.
- Spitzer, W.G., Miller, R.C., Kleinman, S.A., and Howarth, L.E. (1962) Far infrared dielectric dispersion in BaTiO_3 , SrTiO_3 , and TiO_2 . *Physical Review*, 126, 1710–1721.
- Sinclair, W., and Ringwood, A.E. (1978) Single crystal analysis of the structure of stishovite. *Nature*, 272, 714–715.
- Striefler, M.E., and Barsch, G.R. (1976) Elastic and optical properties of stishovite. *Journal of Geophysical Research*, 81, 2453–2466.
- Summit, R. (1968) Infrared absorption in single-crystal stannic oxide: Optical Lattice-vibration modes. *Journal of Applied Physics*, 39, 3762–3767.
- Traylor, J.G., Smith, H.G., Nicklow, R.M., and Wilkinson, M.W. (1971) Lattice dynamics of rutile. *Physical Review B*, 10, 3457–3472.
- Weidner, D.J., Bass, J.D., Ringwood, A., and Sinclair, W. (1982) The single-crystal elastic moduli of stishovite. *Journal of Geophysical Research*, 87, 4740–4746.
- Wyckoff, R.W.G. (1965) *Crystal structures*. John Wiley and Sons, New York.

MANUSCRIPT RECEIVED JANUARY 30, 1990

MANUSCRIPT ACCEPTED FEBRUARY 20, 1990